The detection of lung cancer using MTANN (Massive Training Artificial Neural Network) based soft tissue technique

Kishore Rajagopalan (kishoreresearchscholar@gmail.com)
Kamaraj College of Engineering and Technology https://orcid.org/0000-0002-5617-5307
Suresh babu
Kamaraj College of Engineering and Technology

Technical advance

Keywords: x-ray, sensitivity, lung cancer

Posted Date: April 29th, 2020

DOI: https://doi.org/10.21203/rs.3.rs-25307/v1

Version of Record: A version of this preprint was published on October 31st, 2020. See the published version at https://doi.org/10.1186/s12911-020-01220-z.

The detection of lung cancer using MTANN (Massive Training Artificial Neural Network) based soft tissue technique

Abstract

Background: An existing computer aided detection (CAD) [31] scheme faces major issues during subtle nodule recognition. However, radiologists have not noticed subtle nodules in beginning stage of lung cancer. **Method:** In the proposed computer aided detection (CAD) system, this issue has been resolved by creating MTANN based soft tissue technique from the lung segmented x-ray image. X-ray images are downloaded using JSRT(Japanese society of radiological technology) image set. JSRT image set includes 233 images (140 nodule x-ray images and 93 normal x-ray images). A mean size for a nodule is 17.8 mm and it is validated with computed tomography (CT) image. Thirty percent (42/140) abnormal represent subtle nodules and it is split into five stages (tremendously subtle, very subtle, subtle, observable, relatively observable) by radiologists. **Result:** An existing computer aided detection (CAD) [31] scheme attained 66.42% (93/140) sensitivity having 2.5 false positives (FPs) per image. Utilizing MTANN based soft tissue technique, many nodules superimposed by ribs as well as clavicles have identified (sensitivity is 72.85% (102/140) at one false positive rate). **Conclusion**: In particular, proposed computer aided detection (CAD) system using soft tissue technique determine sensitivity in support of subtle nodules (14/42=33.33%) is statistically higher than CAD (13/42=30.95%) [31] scheme without soft tissue technique. A proposed CAD scheme attained tremendously minimum false positive rate and it is a promising technique in support of cancerous recognition.

Keywords: x-ray, sensitivity, lung cancer

1 Background

1.1 General

Cells [1] were vital units in our lung region, which were having its unique framework. Cancer [2] is a syndrome which might appear as an increased abnormal cell uncontrollably. However, it happens across any portion of a body [5]. So, it results in the change in genetic behavior [5] which deter the regular flow (cell may fabricate new cells during early stages and it dies while they were growing old). It might have a possibility for producing tumors in the lymphatic system. Doctors partition cancer into categories based on its foundation. The categories were listed as Carcinomas, Sarcomas, Leukemias as well as Lymphomas [3] [4]. Table 1.1 [7] indicates a list of cancer types available in all over the world with its 5 year survival rate.

Table 1.1 lists of cancer types and their five year endurance rate

Type of cancer	five year endurance rate
Oral cancer	60%
Lip cancer	91%
Hypopharynx cancer	33%
Heart cancer	10%
Esophageal cancer	19%
Stomach cancer	30.6%
Small Intestine cancer	67.5%
Gall bladder cancer	18.2%
Lung cancer	18.1%
Bone cancer	67.7%
Breast cancer	89.7%
Cervical cancer	67.1%
Prostate cancer	98.6%
Brain cancer	33%
Myeloma	49.9%
Non lymphoma lymph node cancer	48%
Leukemia	68.2%
Thyroid Cancer	98.2%
Colorectal cancer	64.9%
Laryngeal cancer	60.7%
Uterine cancer	29.8%-82.7%
Ovarian cancer	46.5%
Ocular cancer	82.7%
Glioblastoma	19%
Appendix cancer	88%
Skin cancer	91.7%
Testicular cancer	95.1%
Hodgkin's lymphoma	86.4%
Non-Hodgkin's lymphoma	71%
Pancreatic cancer	8.2%
Pancreatic neuro endocrine tumor	61%

Cancer with particular category does not produce tumors, which was leukemias, various lymphoma types and myeloma. Tumor sites are listed here: gastric, colorectal, esophageal, pancreatic, breast, cervical, lung as well as prostate [6]. Among these tumor sites, lung tumor has hazardous one. The most significant utility for lung was holding a stream utilizing oxygen within the entire body. However, blood flow was interrupted through these tumors.

Lung cancer is a single hazardous syndrome, which might present in small as well as non small cell [9]. Lung cancer recognition in premature phase has no symptom. Premature stage lung nodule recognition has represented at Fig 1.1 However, during this stage, the root cause has not well known. Once doctors discovered root cause has been ignored by the patient, which result in late diagnosis and further treatment. Nodules seen within an x-ray image might not essentially be lung cancer, it reports an abnormality which was specified as pneumonia, tuberculosis or calcified granuloma. So, it was a tedious work for radiologists during the past few decades. Lung nodule widens towards the chest center since natural lobe situated across the lung region needs to be known earlier [9]. However, it is a exigent task of radiologists since ribs and clavicles are being overlapped with it. X-ray utilize few energy with direction in obtaining imagery rooted in body's interior structure. They are frequently accustomed toward assisting with identifying cracked bone, glance for wound or infection and to find a strange object in soft tissue. These might utilize an iodine-based contrast material or barium to build up the visibility of specific organ, blood vessels, tissues or bone. So, it has been used to identify chest syndromes because they are most cost-effective, routinely available and dose-effective diagnostics. However, X-ray images are suited for the improvement done in the image processing technique which does not need iodine-based contrast material to pick up the visibility of a specific organ. Hence, 30% nodules in x ray image are missed by radiologists and that, 82-95% missed nodules are partly obscured by overlying bone such as ribs and clavicles [10] [11]. For solving the issue of detecting nodule which is overlapping with ribs and clavicles, we proposed a novel CAD scheme of MTANN based soft tissue technique.

1.2 Related works

J.S. Lin [12] used two level neural classifiers for reducing false positive through computer aided analysis. However, lung tumor was recognized with ladder structured decision trees [13]. A co-occurrence matrix using texture measures [14] has been utilized for lung nodule detection. Most ordinary problems encountered throughout nodule finding was overlapping rib and clavicle with a nodule. When we utilize an overlapped image, it was difficult in detecting a suspicious area. Several imaging techniques have been proposed during recent literature review such as analyzing texture, watershed segmentation [15], Gaussian filters [16], active shape modeling [17] and quasi-Gabo filters [18]. In [19], feature sets hold translation invariant wavelet with co-occurrence mammogram attributes were used in image categorization. Features extracted from multi scale Gaussian filter bank and some specific features that were readily calculated from blob detector scheme to detect nodules [20]. Local curvature using image data was considered when viewed using relief map [21].

Matsumoto et. al., proposed computer aided detection scheme using x-ray images at 11 false positive rates, even though the system had 80% sensitivity. But lung nodule detection accuracy was not improved [22]. Feng Li et. al. [23] detects small lung cancers in x-ray image for false positive reduction. This would increase their confidence level of radiologist by utilizing dual energy subtraction technique. However, using such technique requires specialized equipments and dual energy images are prone to motion artifact.

Existing computer aided detection scheme known as most efficient tool since it was missing lung nodule due to overlapping rib. To address this problem, dual energy subtraction strategies using radiation exposures [24] were considered for decomposing a radiograph into bone-free and soft tissue free image. So, it had been widely accepted in clinical practice because its clinical value can improve diagnostic efficiency. However, there were problems such as high radiation dose and motion artifacts due to double exposure with different energies. This problem had been addressed by using deep learning [25] .Deep Learning has assumed that there was a nonlinear relationship between dual energy image. If the nonlinear relationship was deduced using deep learning, a dual energy image could be generated from single energy chest radiography without double exposures. They had utilized chest radiograms in training (lung image database consortium (LIDC-IDRI)) database [25]. Their training data utilized in this study were a single energy and dual energy chest radiogram pair. They utilized single energy chest radiogram and dual energy soft tissue free image. Deep learning model is a U-net based model and they added a shortcut connection between convolution layers. To optimize such a learning model, they had utilized the adaptive momentary estimation (ADAM) optimization method.

The virtual dual energy [25] bone free chest radiogram was obtained by subtracting the predicted dual energy soft tissue free chest radiograms from the conventional single energy chest radiogram. Kenji Suzuki developed pixel based device mechanism using medical image processing

which avoids error caused by inaccurate feature calculation and segmentation while classifying objects into certain classes [26].Takeshi Kobayashi, Xin-Wei Xu, Heber MacMahon, Charles E. Metz, Kunio Doi evaluate the consequence on nodule output by utilizing ROC analysis with two diverse techniques involved in computer aided diagnosis scheme [27]. Donghoon Lee, Hwiyoung Kim, Byungwook Choi, Hee-Joung Kim developed a deep learning which reduces double exposure with improvement of diagnostic accuracy [28].

In this work, MTANN based soft tissue technique has been expanded with JSRT image set in support of subtle nodule recognition. it will facilitate a proposed computer aided detection scheme without double x-ray exposures.. It will enable maturing a proposed computer aided detection scheme without double X-ray exposures.

2 Methods

2.1 Database of X-ray image

A 247 image set has been downloaded from the Japanese Society of Radiological Technology (JSRT) [30]. From that, 140 abnormal and 93 normal images were selected. Detail is made available in Table 2.1

Selected images have been subjected to nodule detection with absence in opaque portions. These sizes were 2048 x 2048 pixels. All nodules in this database were validated by computed tomography and their location was verified by chest radiologists. A digitized image having 12 bits with a pixel quality of 2048 x 2048. A pixel size was 0.175 x 0.175 mm. Subtle nodule may be divided into five stages which are tremendously subtle, very subtle, subtle, observable, relatively observable.

A MTANN based soft tissue technique has been created for discerning precise opacity from other opacities in chest radiography. So, it is utilized to differentiate subtle nodules. This technique was required when it has acquired equipping image by rib suppression and was evaluated by 233 images. The allotment of nodules in the JRST database was based on it's size and précised in Table 2.1 Shiraishi et al. [30] have eliminated cases in this study comprising lung nodule in opaque scenarios for x-ray image that match up to the retro-cardiac as well as sub-diaphragmatic areas of the lung. However, 7.6% (76/1000) of these scenarios belong to these areas. Opaque scenarios represent 9.1% (14/154) of the JRST dataset

Table 2.1 Allotment of nodules in the JRST database based on nodule size

	Size(mm) categories			
	Small	Medium	Large	Total
Tremendously subtle	2	18	5	25 (16.2%)
Very subtle	3	16	10	29 (18.8%)
subtle	4	29	17	50 (32.5%)
Relatively observable	1	20	17	38 (24.7%)
observable	0	5	7	12 (7.8%)
Pathology				
Benign	7	34	13	54
Malignant	3	54	43	100

2.2 Existing computer aided detection scheme

At a University of Chicago Hospital in a Department of Radiology [32], x-rays were acquired utilizing a single exposure based dual energy radiography system. Original image dimensions was 1760 x 1760. This dimension is reduced to 512 x 512 by utilizing sub sampling for a considerable decrease in computation time [17].

2.2.1 Overview

First module employs an imaging pipeline [31] which contains lung separation from other arrangements by utilizing x-ray with an area being suspected as an abnormality. With this module, the system extracts 65x65 square areas for considering suspicious point positioned within middle area. Because it employs pixel-based method, every pixel situated in square area were believed as system inputs. The intensity values fall within these inputs were extorted and stored in a database was utilized to train system at second module. The database was alienated into a number of subcategories, and the information offered in these subcategories would be utilized for the training as well as for testing the results. In a second module, neural network was equipped through input categories which are named as statistical feature based inputs and pixel based inputs.

An existing computer aided detection scheme include four major steps which is represented in Fig 2.1: A) pre-processing B) Binary image conversion and connected component analysis C) feature extortion D) classification.

It contains two modules which were depicted inside Fig 2.1

A) Pre-processing

When they utilized median filtering technique during preprocessing step, the poor contrast effect had eliminated. A low frequency image was created by substituting pixel value with median pixel value over a square area as 5x5 pixel centered at pixel location. Sharpening and histogram equalization techniques were utilized in direction of enhancing image contrast.

B) Binary image conversion and connected component analysis

Binary image conversion has been done to make a computation apt for threshold procedure. By utilizing threshold image, lung masks were prepared through active shape models. However, these masks may be utilized in the connected component analysis during scope identification while user selecting suspicious points [31]. So, lung mask was utilized to group pixel region as an element. i.e., every pixel region having a related element was related to each other

The criterion for x-ray image enclosure using JSRT image set were: (1) nodule absence bigger than 35 mm, (2) suspicious nodule absence that were not launched by CT examination, and (3) nodule absence with margin that might not be established by a radiologist. The subtlety holded within this image set are clustered into five categories, namely, observable, relatively observable, subtle, very subtle and tremendously subtle. These categories have been described by expert radiologists which takes into account size, contrast, and anatomical position of lesion.

C) Feature Extortion

14 features were extorted from the above method (Binary image conversion and connected component analysis) and listed in Table 2.2

Table 2.2 Features extorted using existing computer aided detection scheme

S.No.	Extorted feature
1	Contrast value
2	Correlation value
3	Energy value
4	Homogeneity value
5	Gray level
6	Mean
7	Standard Deviation
8	Entropy
9	Circularity
10	Uniformity
11	Smoothness of the intensity
12	Skewness of the histogram
13	Area
14	Perimeter

The circular index of each connected module M_i is defined as

$M_i = 4\pi A_i/R_i^2$ ----------(1)

where A_i is the area (nodule) of each image in JSRT image set, R_i is the perimeter (nodule) of each image in JSRT image set. It is calculated based on the area and the perimeter. If a connected module exhibits a circular index nearer to 1, then there is a high probability of nodule consideration.

After recognizing a region that illustrates a high probability of being a nodule, this scheme proceed to the second phase of their algorithm to train the classification.

D) Classification

A neural network having one hidden layer of 1000 neurons and an input layer of 10 neurons to hold the first and second order textures were utilized at the training phase. Based on the utilization of the training phase, subtle nodules were grouped into five categories which are named as observable, relatively observable, subtle, very subtle and tremendously subtle. It is based on size, contrast, and anatomical position of the nodule.

2.3 Creation of MTANN based soft tissue technique

In the radiography field, MTANN filter was involved. However, this was vital to discriminate precise opacity from other opacities. Soft tissue technique was created (described in equation 9) by utilizing x ray. It was used as rib and clavicle suppressed [41] form. Fig 2.2 show soft tissue technique creation using x-ray. MTANN [42], a nonlinear filter which needs to be trained with x ray image and training image. The bone image has been obtained without usage of specialized equipments were utilized as

equipping image. Equation (2) represents a mapping of input vector utilizing neural network.

The MTANN contain linear-output ANN regression model which is able to handle image data directly.

$$f(u,v) = NN(\vec{a}_{u,v}) \quad \text{----------(2)}$$

Where $\vec{a}_{u,v} = \{g(u-i,v-j) \mid u-i, v-j \in R_s\}$ is an input vector to MTANN which represent sub region, f(u,v) represent an estimate of a teaching value. Equation (3) represents an actual function of rib suppression between input vectors and training values. R_s and R_t denote sub and training region.

$$\{\vec{a}(u,v), T(u,v) \mid u,v \in R_T\}$$

$$= \{(a_1,T_1)(a_2,T_2) \ldots\ldots (a_N,T_N)\} \quad \text{----------(3)}$$

Where T (u, v) is a training image and N is pixel number in training region.. For a sole MTANN, rib holding different frequencies maintains complex suppression due to limited ability. With an intention of conquering this issue, multi resolution decomposition/composition techniques were applied. First lower resolution image G_L (u, v) acquired from higher resolution image G_H (2u, 2v) by executing down sampling with average, i.e., four pixels replaced by a mean value of four pixels represented by an equation (4)

$$G_L(u,v) = (1/4) \sum_{u,v \in R_{22}} G_H(2u-i, 2v-j) \quad \text{----------(4)}$$

Where R_{22} represent 2 x 2 region. The lower resolution area replaced four regions having the same value through up sampling, were represented in an equation (5) as follows:

$$G_L^U(u,v) = G_L(u/2, v/2) \quad \text{-------(5)}$$

$$S = G_L^U(u,v) \quad \text{----------(6)}$$

Then, enlarged lower resolution region is subtracted from higher resolution region shown in equation (6) and (7)

$$D_H(u,v) = G_H(u,v) - S \quad \text{----------(7)}$$

This procedure was performed uninterruptedly in the lower resolution area. Thus, multi resolution area was crafted by using a multi resolution decomposition method. A vital asset of this method is as same as high resolution area G_H (u,v) is acquired in equation (8) is as follows:

$$G_H(u,v) = S + D_H(u,v) \quad \text{----------(8)}$$

As a result, preference will be given to multi resolution region. After training of soft tissue technique, x-ray image

produces bone area which was similar as training bone area. The bone area $f_b(u,v)$ was created from training neural network. Along with it, lung masking area n(u,v) and weighting parameter w_c which was subtracted from the sub region g(u,v) to create soft tissue in equation (9).

$$f(u,v) = g(u-i,v-j) - w_c \times f_b(u,v) \times n(u,v) \quad \text{----------(9)}$$

Where f(u,v) denotes the soft tissue having different types of rib contrast using weighting parameter w_c.

To diminish rib-induced false positive and discern nodule overlapping ribs and clavicles, we have included MTANN based soft tissue technique within a proposed computer aided detection scheme.

Major issues faced during existing computer aided detection scheme was toward discerning nodule superimposed with ribs, rib crossings, and clavicles. During rib as well as clavicle suppression in x-ray image, some nodule candidate has missed by soft tissue technique. We identified those nodule candidates which was done for non subtle nodule within x-ray image through the following steps A) lung field extortion utilizing multi-division active shape model (M-ASM) B) region of interest based on an abnormal identification by utilizing clustering watershed technique C) feature extortion D) classification. During this scenario, sensitivity of proposed computer aided detection scheme is lower than the sensitivity of existing computer aided detection scheme for non subtle nodules. However, sensitivity of existing computer aided detection scheme has progressed by minimum improvement.

2.4 Proposed computer aided detection scheme

Fig 2.3 demonstrates proposed computer aided detection scheme. It incorporates 4 steps: A) lung field extortion utilizing multi-division active shape model (M-ASM) B) region extortion based on an abnormal identification by utilizing clustering watershed method C) feature extortion D) an abnormal categorization utilizing support vector machine.

A) Lung field extortion utilizing multi-division active shape model (M-ASM)

Multi-division active shape model (M-ASM) [35] were permitted during lung field extortion for structural boundary. It determines multiple segments called heart, aorta as well as rib-cage. The node specified active shape

model was discovered through each segment for a particular boundary which resulted in a marked improvement in boundary accuracy. After lung field extortion, background trend correction technique based on second order bivariate polynomial function was employed using equation (10)

$$F(x, y) = ax^2+by^2+cxy+dx+ey+f \text{ ----------(10)}$$

where a, b, c, d, e ,f are co-efficients and F (x, y) denotes an image. In this, x and y indicate pixel co-ordinates.

Segmented lung field image applies different gray level morphological open operation [37] forming nodule enhanced images and a nodule enhanced image have modified likelihood map. MTANN based soft tissue technique have created after lung field segmentation to suppress rib and clavicle in x-ray image. In Fig 2.2, a soft tissue image recognized nodule candidate by utilizing two step nodule enhancement technique (which was done for subtle nodules). Region of interest have identified using soft tissue and x-ray image and feature based on these images [26] [27] are effective. Some nodule had related bone feature, i.e., shape, size, contrast, orientation. However, these features were suppressed using this technique. Due to suppressed feature, identified nodule may be misinterpreted as non nodule in the soft tissue image. To identify such misinterpretation, same feature set may be extorted at the equivalent location in x-ray image.

B) Region extortion based on an abnormal identification by utilizing clustering watershed method

Region of interest was identified based on an abnormality by utilizing clustering watershed technique [20] after lung field segmentation. By utilizing a clustering watershed technique [37], the jagged abnormal area was segmented using multiple catchment basin. Every least point was enclosed by it; thus, there were one or more peaks, each of which was included by a cluster of associated pixels that comprised a catchment basin. From the multiple catchment basin, a single abnormal area was concluded by following clustering method: first, primary cluster was included abnormal location (as a point) decided by initial identification step. Next, clusters connected to primary cluster were inserted. Attached clusters were recognized through utilizing least value between peaks in primary cluster

C) Feature Extortion

Sixty two morphological and gray-level-based features [38] were extorted from the region of interest through x-ray and soft tissue image. The features extorted from x-ray and soft tissue image using proposed computer aided detection scheme were listed in Table 2.3

Table 2.3: Features values from x-ray and soft tissue image using proposed computer aided detection scheme

Feature Extortion	Values in x-ray image	Values in soft tissue image
can.u	6	7
can.v	7.5	8.5
$can.Grad_1$	4.5	5.5
$can.CV_1$	0.65	0.75
$can.Grad_2$	6.7	7.7
$can.CV_2$	7.2	8.2
$Shape_1$	7	8
$Shape_2$	6.6	7.6
$Shape_4$	5.8	6.8
$Gray_1$	7	8
$Gray_2$	8.2	9.2
$Gray_3$	8.4	9.4
$Gray_4$	9.2	8.2
$Gray_5$	7	8
$Gray_6$	8.2	9.2
$Gray_7$	8.4	9.4
$Gray_8$	9.2	9.2
$Grad_1$	37	47
$Grad_2$	30	40
$Grad_3$	1.23	1.175
$Surface_1$	25	35
$Surface_2$	27	37
$Surface_3$	675	1295
$Texture_1$	30	40
$Texture_2$	32	42
$Texture_3$	34	44
$Texture_4$	36	46
$Texture_5$	38	48
$Texture_6$	40	50
False Positive	2.5	1

D) Classification

After nodule area extortion, feature extortion have given as an attempt to non linear support vector machine [39] (SVM) for categorizing abnormality. Based on feature extortion, a common size of an abnormal area (17.8 mm) was detected.

3. Results

Here, proposed computer aided detection scheme has been demonstrated. First, MTANN based soft tissue technique was created. Next, the soft tissue image having different rib contrast was plotted using sensitivity in favor of finding

peak value.

3.1 MTANN based soft tissue technique training

Four images from JSRT database have used to train MTANN. one was normal while other three were abnormal. In Fig 2.3, massive training artificial neural network size has 9 x 9 pixels.

It was enough to wrap rib width in image. Three layered, massive training artificial neural network was utilized to restrain rib where input, hidden and output units was 81, 20 and 1 respectively. Fig 3.1 demonstrates plotted rib contrast values using soft tissue images. It is explained in the next section.

3.2 Nodule candidate identification

We subtract bone image from the novel x-ray image as per equation (10) in Section 2.3. From this, we obtain a soft tissue image. There was a factor Mc to regulate rib disparity in soft tissue images. A rib disparity is a factor obtain from a different soft tissue image by the use of the weighting parameter(equation (10)) and it's range lies between 0 and 1. In Fig 3.1, highest sensitivity value (95%) is concluded while rib (contrast) parameter M_c was 0.4. As in soft tissue image, most nodules were identified in different rib contrast during a candidate identification step. In a plotted graph, 84% candidates have max code (nodule likelihood) values represent probability map were utilized toward an origin point. The nodule candidate identification in MTANN based soft tissue technique utilizing JSRT image set was achieved 95% (135/140) sensitivity. In Fig 3.2, Number of false positives per image vs Sensitivity were plotted. False positive of 1 were obtained by using 84% sensitivity for 154 nodule images. The values of features extracted from x-ray and soft tissue image using proposed computer aided detection scheme are shown in Table 2.3

Table 3.1 indicates a sensitivity and false positive of several computer aided detection schemes which was utilized JSRT image set. Wei et al. [49] gave information about their CAD scheme which attained 80% sensitivity and 5.4 FPs per image by means of utilizing JSRT database. Due to large amounts of false positive (5.4), radiologist accuracy in identifying lung nodule was not progressed. Hardie.,et. al., gave information about their CAD schemes which was marked 63% nodules in JSRT image set and 2 FPs per image [55]. Their concert was considered by utilizing 25 mm distance decision for finding out true positive (TP) recognitions. concert of our CAD system with MTANN based soft tissue technique (72.85%) has substantially higher than Chen reported scheme [64].

4. Discussion

By utilizing dual-energy subtraction [23] [24] technique, it was very complex task in the direction of gathering larger radiation dose. MTANN based soft tissue technique has the possibility toward improving sensitivity with specificity which was buried as a consequence of suppressing rib with a discriminating nodule contained by an another regular anatomic structure. For an obscuring bone, single exposure based dual energy subtraction technique [62] had addressed. By utilizing this technique, the soft-tissue image was produced. When we use this technique, sensitivity was improved. By using these benefits, a fixed number of hospitals utilize radiography systems by dual-energy subtraction, because dedicated tools for acquiring dual-energy X-ray exposures [28] was required.

In our approach, MTANN based soft tissue technique was utilized in direction for building soft tissue image. It was trained using four x-ray images (one was a normal image while other three was nodule image) from JSRT image set. Highest rib contrast factor has been observed. We utilize this trained x-ray on behalf of restraining ribs and clavicles. But, their result has not optimized. If we test x-ray image, it may have a better show. To facilitate this issue, some nodules have concealed. In a proposed computer aided detection scheme, MTANN based soft tissue technique integrated 2 diverse images (bone, x-ray image) together and extorted feature set using soft tissue image after lung field segmentation. In this paper, MTANN based soft tissue technique has been projected. As within x-ray image, we observe nodule candidate during rib contrast parameter variation. During this technique, a constant rib contrast factor was preferred which was represented as maximum peak in feature recognition in favor of every abnormal cases utilizing JSRT image set.

Abbreviation: CAD, MTANN, JSRT, FP

Table 3.1 Performance comparison of several existing computer aided detection systems which used JSRT Database

	Sensitivity	FPs/image	Methodology	Classifier	Database
Wei et al.[49]	80% (123/154)	5.4 (1333/247) (less accuracy due to high FPs)	Forward stepwise selection	Fisher linear discriminant	All abnormal as well as normal image inside JSRT(247)
Coppini et al. [58]	60% (93/154)	4.3 (662/154)	Neural network filter	Fisher linear discriminant	All nodule image in JSRT(154)
Schilham et al [17]	51% (79/154) 67% (103/154)	2 (308/154) 4 (616/154)	Image filtering Based on Regression	Fisher linear discriminant	All nodule image in JSRT(154)
Hardie et.al. [55]	80% (112/140) 63% (88/140)	5.0 (700/140) 2 (280/140)	Active shape model and new weighted multi-scale conver gence-index	Fisher linear discriminant	Nodule image in JSRT(140)
Chen et.al. [64]	71% (100/140)	2 (466/233)	Computer aided detection using neural filter	Support Vector Machine (SVM)	Nodule and Normal image in JSRT(233)
Proposed MTANN based soft tissue technique	72.85% (102/140)	1 (233/233)	MTANN for rib suppression	Support Vector Machine (SVM)	Nodule and normal image in JSRT(233)

5. Declarations

Ethics approval and consent to participate:
http://www.biomedcentral.com/about/editorialpolicies#Ethics

Consent for publication: yes

Availability of data and materials:
http://www.biomedcentral.com/submissions/editorial-policies#availability+of+data+and+materials

Competing interests: no

funding: no funding received

Authors Contributions: The authors have declared that there is no conflict of interest

6. Conclusion

Here, the proposed computer aided detection (CAD) scheme using MTANN based soft tissue technique is being

widened as 72.85% sensitivity after sub region identification. Hence, the subtle nodule was detected using a non linear filter. In this work, the nonlinear filter was MTANN. It is a promising method for radiologists to recognize an abnormality by x-ray images from JSRT image set. By utilizing MTANN filter, false positive of the proposed CAD scheme have diminished to 1 which was lower than previous works

Acknowledgements:
We will give our sincere thanks to Kamaraj College of Engineering and Technology, Virudhunagar, India for doing this research work in the Department of Electronics and Communication Engineering.

Our special thanks to Dr. Anant Achary, M.Tech., Ph.D., Principal, Kamaraj college of Engineering and Technology, Virudhunagar, India for his encouragement and continuous support for this research work.

Our regards to Dr. Joe Pradeep Kumar, MBBS, Indian MRI Diagnostic & Research Limited, Madurai for his guidance and validation of data.

7. References

[1] https://www.cancer.net/

[2] https://www.healthline.com

[3] American Cancer Society, American Cancer Society Complete Guide to Complementary and Alternative Cancer Therapies, 2nd ed.Atlanta (2002), GA.. American Cancer Society.

[4] https://www.medicalnewstoday.com/articles/323648

[5] Tsuyoshi Okuhara, Hirono Ishikawa, Akiko Urakubo, Masayo Hayakawa, Chikako Yamaki, Tomoko Takayama, Takahiro Kiuchi, “Cancer information needs according to cancer type: A content analysis of data from Japan’s largest cancer information website”, Preventive Medicine Reorts, 2018

[6] en.wikipedia.org

[7] moziani.tripod.com

[8] Brian Tzung. "Lung Cancer Screening", Medical Management of the Thoracic Surgery Patient, 2010

[9] C.I. Henschke, D.I. McCauley, D.F. Yankelevitz, D.P. Naidieh, G.McGuinness, O.S Miettinen, D.M. Libby, M.W. Pasmantier, J. Koizumi, N.K. Altorki, J.P. Smith, “Early lung cancer action project: Overall design and findings from baseline screening”, Lancet(1999), vol. 354, pp. 99-105.

[10] J.H Austin, B. M. Romney, L.S Goldsmith, Missed bronchogenic carcinoma: Radiographic findings in 27 patients with a potentially resectable leison evident in reterospect, Radiology(1992), vol. 182, pp 115-122.

[11] P. K. Shah, J. H. Austin, C. S. White, P. Patel, L. B. Haramati, G. D. Pearson, M. C. Shiau, and Y. M. Berkmen,Missed non-small cell lung cancer: Radiographic findings of potentially resectable lesions evident only in retrospect”, Radiology(2003), vol. 226, pp. 235–241.

[12] J.S. Lin, S.B. Lo, A. Hasegawa, M.T. Freedman and S.K. Mun, Reduction of false positives in lung nodule detection using a two-level neural classification, IEEE Trans. on Medical Imaging(1996), vol. 15, pp. 206-216.

[13] Ballard, Sklansky, A Ladder Structured Decision Tree for Recognizing Tumors in Chest Radiographs”, IEEE Transactions on Computers(1976), vol. C-25, issue: 5, pp. 503-513.

[14] G.S. Cox, F.J. Hoare and G. de Jager, Experiments in lung cancer nodule detection using texture analysis and neural network classifiers, Third South African Workshop on Pattern Recognition, 1992

[15] K. Le, Automated detection of early lung cancer and tuberculosis based on X-ray image analysis, Proc. WSEAS International Conference on Signal, Speech and Image Processing, pp. 1-6, 2006.

[16] P. Campadelli, E. Casiraghi and D. Artioli, A fully automated method for lung nodule detection from postero-anterior chest radiographs, IEEE Trans. on Medical Imaging, vol.25, N 12, pp. 1588-1602, 2006

[17] A.M.R. Schilham, B.V. Ginneken and M. Loog, A computer-aided diagnosis system for detection of lung nodules in chest radiographs with an evaluation on a public database, Medical Image Analysis, vol. 10, N 2, pp. 247-258, 2006.

[18] M. Park, J. S. Jin and L. S. Wilson, Detection of abnormal texture in chest X-rays with reduction of ribs, Proc. Pan-Sydney area workshop on visual information processing,2004.

[19] L. Zhang and X. Gao, Research on translation invariant wavelet transform for classification in mammograms, Proc. 3rd international conference on natural computation, 2007.

[20] S.B. Lo, S.L. Lou, J.S. Lin, M.T. Freedman and S.K. Mun, Artificial convolution neural network techniques and applications for lung nodule detection, IEEE Trans. on Medical Imaging, vol. 14, pp. 711-718, 1995.

[21] R. Hayashibe, N. Asano, H. Hirohata, K. Okumura, S. Kondo, S. Handa, M. Takizawa, S.Sone and S. Oshita, An automatic lung cancer detection from X-ray images obtained through yearly serial mass survey, Proc. International conference on image processing,pp. 343 - 346, 1996.

[22] T. Matsumoto, K. Doi, A. Kano, H. Nakamura, T. Nakanishi, “Evaluation of the potential benefit of computer aided diagnosis (CAD) for lung cancer screenings using photofluorography: analysis of an observer study”, Nihon Igaku Hoshasen Gakkai Zasshi(1993), vol. 53, pp. 1195 -1207, Oct 25.

[23] F. Li, R. Engelmann, K. Doi, and H. MacMahon, “Improved detection of small lung cancers with dual-energy subtraction chest radiography”, AJR Amer. J Roentgenol (2008), vol.190, pp.886–891.

[24] Farheen Manji, Jiheng Wang, Geoff Norman, Zhou Wang,David Koff, “Comparison of dual energy subtraction chest radiography and traditional chest X-rays in the detection of

pulmonary nodules", Quantitative Imaging in Medicine and Surgery.

[25] Bo zhou, Xunyu lin, Brendan eck, Jun hou, David wilson, "Generation of virtual dual energy images from standard single-shot radiographs using multi-scale and conditional adversarial network", Robotics Institute, School of Computer Science, Carnegie Mellon University, Department of Biomedical Engineering, Case Western Reserve University

[26] Kenji Suzuki, "Pixel-Based Machine Learning in Medical Imaging", International Journal of Biomedical Imaging (2012), Hindawi Publishing Corporation, pp 1-18.

[27] Takeshi Kobayashi, Xin-Wei Xu, Heber MacMahon, Charles E.Metz, Kunio Doi, "Effect of a Computer-aided Diagnosis Scheme on Radiologists Performance in Detection of Lung Nodules on Radiographs", Radiology(1996), pp 843-848.

[28] Donghoon Lee, Hwiyoung Kim, Byungwook Choi, Hee-Joung Kim, "Development of a deep neural network for generating synthetic dual-energy chest X-ray images with single X-ray exposure", Research Institute of Health Science, Physics in Medicine and Biology(2018).

[29] http://db.jsrt.or.jp/eng.php

[30] Shiraishi, J., Li, Q., Suzuki, K., Engelmann, R., Doi, K., Computer aided diagnostic scheme for detection of lung nodules on chest radiographs: Localized search method based on anatomical classification, Medical Physics 33 (7) (2006), 2642–2653.

[31] K.A.G. Udeshani, R.G.N. Meegama, T.G.I. Fernando,"Statistical Feature-based Neural Network Approach for the Detection of Lung Cancer in Chest X-Ray Images",International Journal of Image Processing(2011), pp 425-434

[32] https://radiology.uchicago.edu/about/early-years

[33] Ting Shu, Bob Zhang, Yuan Yan Tang, "An extensive analysis of various texture feature extractors to detect Diabetes Mellitus using facial specific regions", Computers in Biology and Medicine (2017)

[34] Gergely Orban, Gabor Horvath, "Algorithm fusion to improve detection of lung cancer on chest radiographs", International Journal of Intelligent Computing and Cybernetics (2012)

[35] Bram van Ginneken, Alejandro F. Frangi, Joes J. Staal, Bart M.ter Haar Romeny, Max A. Viergever, Active shape model segmentation with optimal features, IEEE Transactions on medical imaging, (2002), Vol.21, No.8.

[36] Haralickv RM, Sternberg SR, Zhuang X, Image analysis using mathematical morphology, IEEE Transactions on Pattern Analysis and Machine Intelligence (1987), pp 532-550.

[37] Lue Vincent, Pierre Soille, "Watersheds in Digital Spaces: An efficient algorithm based on immersion simulations", IEEE Transactions on Pattern Analysis and Machine Intelligence(1991), Vol. 13, No. 6, June.

[38] Lilla Boroczky, Luyin Zhao, K.P. Lee, Feature subset selection for improving the performance of false positive reduction in lung nodule CAD, IEEE symposium on computer based medical systems(2005).

[39] J. P. Egan, G. Z. Greenberg, and A. I. Schulman, "Operating characteristics, signal detectability, and the method of free response" J. Acoust. Soc. Amer.(1961), vol. 33, pp. 993–1007.

[40] Chen S and K Suzuki, "Computerized detection of lung nodules by Means of 'virtual dual energy' Radiography", IEEE Transactions on Biomedical Engineering", 2013.

[41] Kenji Suzuki, Hiroyuki Abe, Heber MacMahon, Kunio Doi, Image processing technique for suppressing ribs in chest radiographs by means of massive training artificial neural network, IEEE Transactions on Medical Imaging(2006), vol.25, no.4.

[42] Hayati Ture, Temel Kayikcioglu, Detection and Segmentation of Nodules in Chest Radiographs Based on Lifetime Approach,© Springer(2017).

[43] Kiroğlu, ""Comparison of segmentation algorithms for detection of hotspots in bone scintigraphy images and effects on CAD systems",Biomedical Research(2017),vol 28, issue 2.

[44] N.S Raghava, G.Senthil Kumar,"Image Processing for Synthesizing Lung Nodules: A Experimental Study", Journal of Applied Sciences(2006), pp 1238-42.

[45] Saleem Iqbal, Khalid Iqbal,Fahim Arif, Arslan Shaukat,Aasia Khanum,"Potential Lung Nodules Identification for Characterization by Variable Multistep Threshold and Shape Indices from CT Images", Computational and Mathematical Methods in Medicine(2014),Hindawi Publishing Corporation.

[46] Suzuki K, Machine Learning in Medical Imaging Before and After Introduction of Deep Learning. Journal of Medical Imaging and Information Science(2017) 34 (2): 14-24.

[47] Inyoung Song, Jeong Geun Y, Jeong Hee Park, Kyung Myung Soo Lee, Myung Jin Chung, "Color radiography in lung nodule detection and characterization: comparison with conventional gray scale radiography",BMC Medical Imaging(2016), pp 1-7.

[48] Janet E. Kuhlman, Jannette Collins, Gregory N. Brooks, Donald R. Yandow, Lynn S. Broderick, "Dual-Energy Subtraction Chest Radiography: What to Look for beyond Calcified Nodules", Radiographics(2006), pp 79-92.

[49] J.Wei, Y.Hagihara, A. Shimizu, H. Kobatake, "Optimal image feature set for detecting lung nodules on chest X-ray images", in Proc. Computer Assisted Radiology Surgery(2002), pp 706-711.

[50] Jiahui Wang, James T Dobbins III, Qiang Li, "Automated lung segmentation in digital chest tomosynthesis", Medical Physics(2012), pp 732-741.

[51] Chunli Qin, Demin Yao, Yonghong Shi, Zhijian Song(2018),"Computer-aided detection in chest radiography based on artificial intelligence: a survey", Biomedical Engineering(2018)

[52] Senthil Kumar TK,Ganesh EN,Umamaheswari R, "Lung nodule volume growth analysis and visualization through auto-cluster k-means segmentation and centroid/shape variance based false nodule elimination",Biomedical Research(2017)

[53] Paola Campadelli, Elena Casiraghi, Simon Columbano, "Lung segmentation and nodule detection in postero anterior chest radiographs", pp 1 -8.

[54] J. Serra, “Image analysis and Mathematical Morphology”, vol 1, New York, Academic(1982)

[55] R. C. Hardie, S. K. Rogers, T.Wilson, and A. Rogers, “Performance analysis of a new computer aided detection system for identifying lung nodules on chest radiographs,” Med. Image Anal., vol. 12, (2008) pp. 240–258.

[56] Shiraishi, J., Li, Q., Suzuki, K., Engelmann, R., Doi, K., Computer aided diagnostic scheme for detection of lung nodules on chest radiographs: Localized search method based on anatomical classification, Medical Physics 33 (7) (2006), 2642–2653.

[57] Nicholas J. Novak, “Does BMI Affect Diagnostic Efficacy of Computer Aided Diagnostic Software in the Identification of Malignant Pulmonary Nodules in Dual Energy Subtracted Chest Radiographs”, (2015) Vol.11, No. 2.

[58] G. Coppini, S. Diciotti, M. Falchini, N. Villari, and G. Valli, “Neural networks for computer-aided diagnosis: Detection of lung nodules in chest radiograms” IEEE Trans. Inf. Technol. Biomed., vol. 7, no. 4, (2003), pp. 344–357.

[59] A. M. Schilham, B. van Ginneken, and M. Loog, “A computer-aided diagnosis system for detection of lung nodules in chest radiographs with an evaluation on a public database,” Med. Image Anal., vol. 10, pp. 247–258, (2006).

[60] Ting Shu, Bob Zhang, Yuan Yan Tang, “An extensive analysis of various texture feature extractors to detect Diabetes Mellitus using facial specific regions”, Computers in Biology and Medicine (2017)

[61] Gergely Orban, Gabor Horvath, “Algorithm fusion to improve detection of lung cancer on chest radiographs”, International Journal of Intelligent Computing and Cybernetics (2012)

[62] Kana Ide, Hiroshi Mogami, Tadashi Murakami, Yoshifumi Yasuhara, Teruhito Mochizuki, ”Detection of lung cancer using single-exposure dual-energy subtraction chest radiography”, Radiation Medicine, volume 25, Article number: 195 (2007)

[63] Chaofeng Li et. al., “False-Positive Reduction on Lung Nodules Detection in Chest Radiographs by Ensemble of Convolutional Neural Networks”, IEEE Access (2018)

[64] S. Chen, K. Suzuki, and H. Mac Mahon, ``Development and evaluation of a computer-aided diagnostic scheme for lung nodule detection in chest radiographs by means of two-stage nodule enhancement with support vector classification," Med. Phys., vol. 38, no. 4, pp. 1844-1858,2011.

[65] www.ijetae.com

[66] Computational Intelligence in Biomedical Imaging, 2014.

[67] www.ajronline.org

[68] “Computer Vision – ACCV 2018”, Springer Science and Business Media LLC, 2019.

Figure Legends

1) fig11.jpg
2) fig21.jpg
3) fig22.jpg
4) fig23.jpg
5) fig31.jpg
6) fig32.jpg

Figures

Fig 1.1 Early stage lung nodule detection

Figure 1

[See figure]

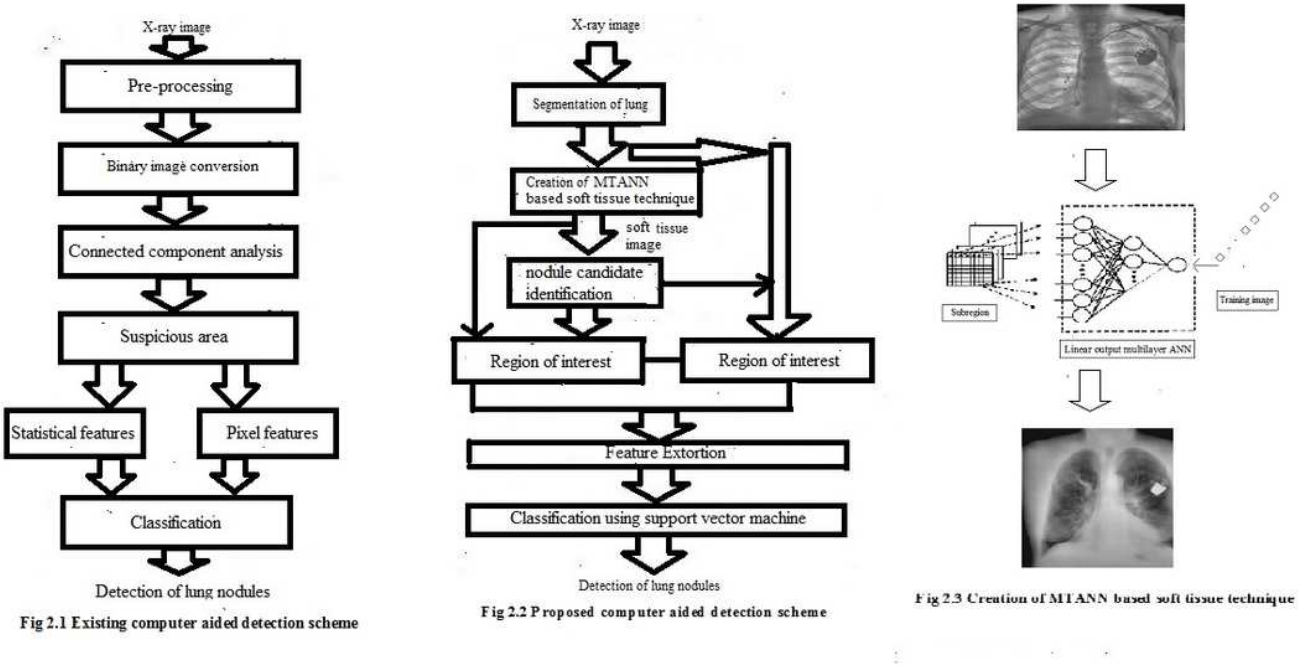

Fig 2.1 Existing computer aided detection scheme

Fig 2.2 Proposed computer aided detection scheme

Fig 2.3 Creation of MTANN based soft tissue technique

Figure 2

[See figure]

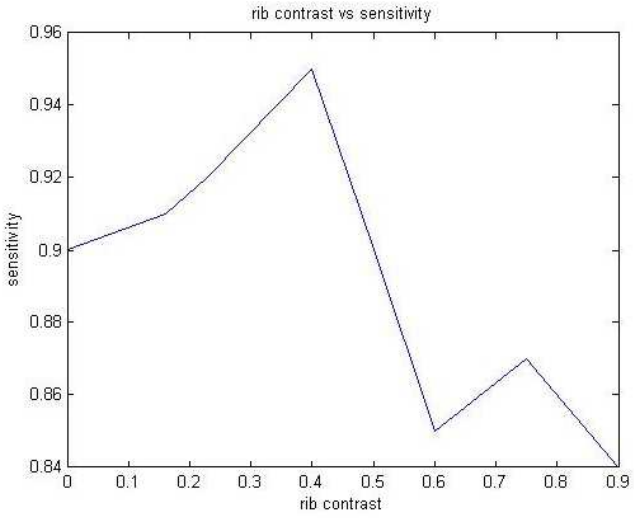

Fig 3.1 rib contrast vs sensitivity

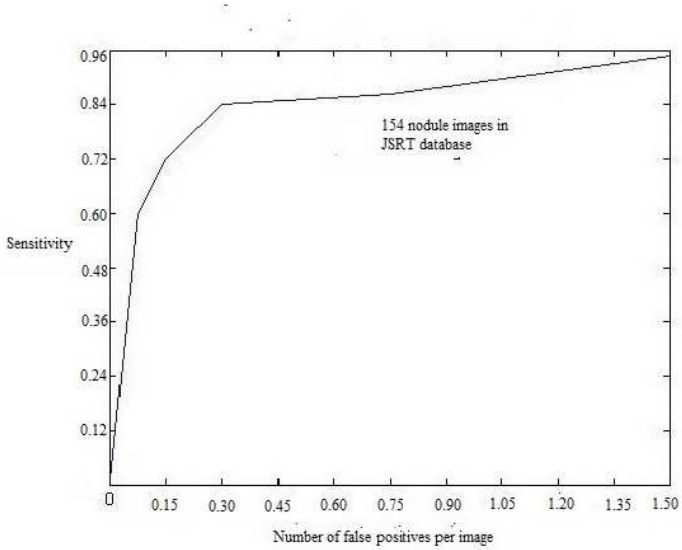

Fig 3.2 Sensitivity vs number of false positives per image

Figure 3

[See figure]